SCIENCE CHINA
Earth Sciences

• RESEARCH PAPER •

May 2015 Vol.58 No.5: 805–814
doi: 10.1007/s11430-014-5022-1

Seismic inversion for underground fractures detection based on effective anisotropy and fluid substitution

CHEN HuaiZhen[1], YIN XingYao[1], GAO JianHu[2], LIU BingYang[2] & ZHANG GuangZhi[1*]

[1] *School of Geosciences, China University of Petroleum, Qingdao 266580, China;*
[2] *Northwest Branch of Research Institute of Petroleum Exploration and Development, PetroChina, Lanzhou 730020, China*

Received July 16, 2014; accepted October 23, 2014; published online December 5, 2014

Underground fractures play an important role in the storage and movement of hydrocarbon fluid. Fracture rock physics has been the useful bridge between fracture parameters and seismic response. In this paper, we aim to use seismic data to predict subsurface fractures based on rock physics. We begin with the construction of fracture rock physics model. Using the model, we may estimate P-wave velocity, S-wave velocity and fracture rock physics parameters. Then we derive a new approximate formula for the analysis of the relationship between fracture rock physics parameters and seismic response, and we also propose the method which uses seismic data to invert the elastic and rock physics parameters of fractured rock. We end with the method verification, which includes using well-logging data to confirm the reliability of fracture rock physics effective model and utilizing real seismic data to validate the applicability of the inversion method. Tests show that the fracture rock physics effective model may be used to estimate velocities and fracture rock physics parameters reliably, and the inversion method is resultful even when the seismic data is added with random noise. Real data test also indicates the inversion method can be applied into the estimation of the elastic and fracture weaknesses parameters in the target area.

rock physics, fractures, seismic inversion, anisotropy

Citation: Chen H Z, Yin X Y, Gao J H, et al. 2015. Seismic inversion for underground fractures detection based on effective anisotropy and fluid substitution. Science China: Earth Sciences, 58: 805−814, doi: 10.1007/s11430-014-5022-1

Subsurface fractures are an important part of the carbonate reservoirs and unconventional reservoirs. Fractures may connect isolated pores, increase the effective porosity of reservoirs, provide path for hydrocarbon migration and improve the permeability. Study shows that subsurface fractures identification which is based on the theory of seismic anisotropy has achieved good application effect (Liu et al., 2012). In addition, Rock physics may build an effective bridge for using seismic data to predict fractured reservoirs. Hence, in this paper, we aim to choose the parameters which are effective for the prediction of underground fractures, and we may use azimuthal seismic data to invert these parameters based on fracture rock physics. We propose a method which utilizes seismic inversion to estimate fracture rock physics parameters directly. This may avoid the errors caused by the conversion of elastic parameters to rock physics parameters. We need to remind that the rock physics parameters are related with fracture parameters (fracture density, fracture fillings, etc.).

There are many studies on fracture rock physics. Nowadays, there are two common rock physics effective models. One is penny-shaped model for cracked media (Hudson, 1981). The other is linear slip deformation (LSD) theory for fractured media (Schoenberg, 1980). The difference between two models is fracture scale. Penny-shaped model assumes that there are thin, penny-shaped ellipsoidal cracks or inclusions in an elastic solid. However LSD model holds

*Corresponding author (email: zhanggz@upc.edu.cn)

that there are discontinuities in a rock and two parts separated by the fracture have rough surfaces. Cheng (1978, 1993) proposed cracked anisotropic effective model, which improved the requirement of crack aspect ratio used in penny-shaped model. Schoenberg et al. (1989) presented layered anisotropic effective model, which assumed the rock containing aligned parallel cracks should be considered as one anisotropic medium. Schoenberg et al. (1995) analyzed the influence of fractures on seismic propagation characteristics, and they thought the rock should contain two parts, isotropic background rock and anisotropic disturbance caused by fractures. Schoenberg et al. (1997) pointed out that layered medium where vertical fractures exist might be equivalent to orthogonal media, and they simulated the characteristics of seismic wave propagation in orthogonal media. Effects of pore fluid on seismic waves may be divided into two areas: Boit (1956a, 1956b) poroelastic wave theory and Gassmann (1951) fluid substitution equation. The former studied the relationship between speed and frequency, but the latter mainly discussed the impact of pore fluid change in seismic frequency. It is well known that seismic wave energy conversion and attenuation may occur when the seismic wave spreads through the rock in which pores are connected by cracks and fractures.

Batzle et al. (1999, 2006) studied the effects of fluid flow and frequency on shear wave velocity, and they showed us the characteristic of velocity and Q factor variation with water saturation and the microscopic mechanism of rock. Chapman (2009) simulated the characteristic of anisotropy affected by multiple sets of meso-scale crack, and he also analyzed velocity variation with azimuth for two cases: open fractures and closed fractures respectively contained in the rock. Quintal et al. (2010a, 2010b, 2011, 2012) showed velocity and seismic attention affected by fluid flow and reflection coefficient variation with water saturation. Tang (2011) presented the development of Boit theory and proposed a cracked porous medium elastic wave theory.

Seismic frequency range is approximately several tens to hundreds of Hz. In this range, we think seismic wave attenuation is small because viscous coupling between the solid and the liquid is well. Hence, we aim to propose a rock physics effective model which is suitable for seismic frequency band. In the model, we research the effect of anisotropy caused by fractures, and we achieve fluid substitution using the formula which also considers the influence of fractures. Brown et al. (1975) proposed a formula for fluid substitution which might be used in anisotropic rock. In our study, we present our effective model, which considers these effects: mineral matrix, pores, cracks and fluid substitution in anisotropic rocks. Using this model, we estimate P- and S-wave velocities and fracture rock physics parameters from well-logging data. The estimation may provide the evidence for seismic inversion, and the estimated fracture rock physics parameters can help to predict the location of fractured layers.

Nowadays, the development of wide-azimuth seismic acquisition and processing makes utilizing seismic data to predict subsurface fractures become a hot research. When fractures are vertically aligned, the rock may be considered to be an equivalent Horizontal Transverse Isotropic (HTI) medium. In order to study the effect of anisotropy on seismic propagation, Thomsen proposed weak anisotropic parameters to describe the degree of anisotropy. Schoenberg et al. (1982) used extended Zoeppritz formula to calculate the accurate result for seismic reflection coefficient. Rüger (1996, 1997, 1998) derived a linearized approximation to the Zoeppritz equation for HTI anisotropy. Studies show that AVO (amplitude variation with offset) analysis has been a useful tool to predict hydrocarbon reservoirs. For HTI media, seismic amplitude varies with incident and azimuthal angles (AVAZ or AVOZ). Hence, it is effective to use azimuthal seismic data to predict underground fractures. One proven method to predict fractures is AVAZ inversion method. Based on Rüger's equation, azimuthal seismic gathers are used to estimate the elastic and anisotropic parameters (Mallick et al., 1998). With the purpose of high-resolution fracture characterization, a new reconstruction of the layer anisotropic elastic parameters was proposed (Bachrach et al., 2009). Downton et al. (2006) presented the uncertainty of using azimuthal seismic data to predict fractures. In our country, there are many studies on carbonate rock reservoir prediction and description. Tang et al. (2002) proposed the method which used the frequency difference to predict fillings in carbonate rock cave, and they applied this method to Tahe oil-field. Yao et al. (2003, 2012) presented a method to detect fractured reservoir, and they also proposed a method to identify caved reservoir by using numerical modeling of wave field. Sa et al. (2011) studied seismic characteristic of fractured reservoir, and they use model and real data to describe the feature of caved reservoir. However, the number of studies on utilizing azimuthal seismic data to estimate fracture rock physics parameters is little. In this paper, we derive a new formula which connects reflection coefficient and fracture rock physics parameters, and propose a method to estimate fracture rock physics parameters directly by using seismic inversion. The introduced rock physics effective model, well-logging data and azimuthal seismic data may increase the accuracy of fractures prediction.

In this paper, we provide the method to predict underground fractures reliably by using azimuthal seismic data. The method begins with rock physics effective model. Using this effective model, we estimate the velocity and fracture weaknesses parameters from the well-logging data. The estimated results may be used as initial constraint for seismic inversion. Using the method, we may predict the anisotropy from well-logging data, and the estimated fracture rock physics parameters can describe the distribution of fractures. This method will be well used in carbonate rock and unconventional reservoirs.

1 Fractured rock physics model and sensibility of fracture weaknesses

To model the response of seismic waves in fractured rock, we use a concept called "equivalent-medium representation" or "effective-medium theory" (Liu et al., 2012). In this paper, we present fractured rock physics model, calculate elastic matrix of fractured rock and estimate P- and S-wave velocities and fracture weaknesses.

1.1 Fractured anisotropic rock physics effective model

The process to build the model may include three parts: the average of mineral, fractured dry rock formation and fluid substitution in anisotropic rock. Figure 1 shows the basis steps of constructing the model. In our study, we select the carbonate rock as the research object.

The details of the model are listed as follows:

Step 1: Estimating the average moduli of the mixture of different minerals (Hill, 1952):

$$M_{VRH} = \frac{M_V + M_R}{2}, \tag{1}$$

where, $M_V = \sum_{i=1}^{N} f_i M_i$, $\frac{1}{M_R} = \sum_{i=1}^{N} \frac{f_i}{M_i}$. M_{VRH}, M_V and M_R may be any moduli, such as bulk modulus, shear modulus or Young's modulus. f_i is bulk modulus of the component, and M_i is elastic modulus of the component.

Step 2: Building non-fractured dry rock model after adding empty intergranular pores using DEM model (Zimmerman, 1991). The formula used to calculate effective bulk modulus K^* and shear modulus μ^* is

$$(1-y)\frac{\mathrm{d}}{\mathrm{d}y}[K^*(y)] = (K_2 - K^*)P^{(*2)}(y), \tag{2a}$$

$$(1-y)\frac{\mathrm{d}}{\mathrm{d}y}[\mu^*(y)] = (\mu_2 - \mu^*)Q^{(*2)}(y), \tag{2b}$$

with initial conditions $K^*(0) = K_1$ and $\mu^*(0) = \mu_1$, where K_1 and μ_1 are the bulk and shear moduli of the intial host material (phase 1), K_2 and μ_2 are the bulk and shear moduli of the incrementally added inclusions (phase 2), and y is the concentration of phase 2. P and Q describe the effect of an inclusion of material.

Step 3: Constructing fractured dry rock model after adding fractures and cracks using linear slip fracture model (Schoenberg et al., 1995). The effective moduli are given as:

$$\boldsymbol{C} = \begin{bmatrix} (\lambda+2\mu)(1-\Delta_N) & \lambda(1-\Delta_N) & \lambda(1-\Delta_N) & 0 & 0 & 0 \\ \lambda(1-\Delta_N) & (\lambda+2\mu)\left(1-\left(\frac{\lambda}{\lambda+2\mu}\right)^2\Delta_N\right) & \lambda\left(1-\frac{\lambda}{\lambda+2\mu}\Delta_N\right) & 0 & 0 & 0 \\ \lambda(1-\Delta_N) & \lambda\left(1-\frac{\lambda}{\lambda+2\mu}\Delta_N\right) & (\lambda+2\mu)\left(1-\left(\frac{\lambda}{\lambda+2\mu}\right)^2\Delta_N\right) & 0 & 0 & 0 \\ 0 & 0 & 0 & \mu & 0 & 0 \\ 0 & 0 & 0 & 0 & \mu(1-\Delta_T) & 0 \\ 0 & 0 & 0 & 0 & 0 & \mu(1-\Delta_T) \end{bmatrix}, \tag{3}$$

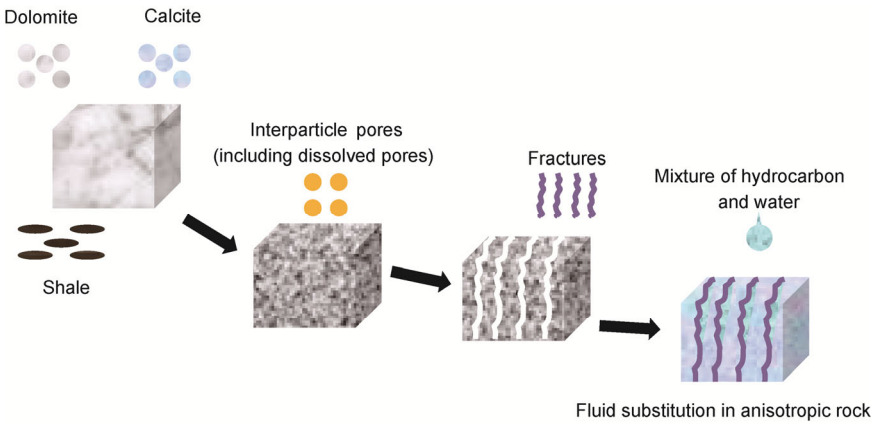

Figure 1 Fractured carbonate rock physics model.

where λ and μ are Lame parameters, Δ_N and Δ_T are the normal and tangential weaknesses. Δ_N and Δ_T are related with the anisotropy of fractured carbonate rock.

Bakulin et al. (2000) made a comparison of Hudson's model and linear slip models. The weaknesses Δ_N and Δ_T can be calculated easily combined with Hudson's model:

$$\Delta_N = \frac{4e}{3g(1-g)\left[1+\frac{1}{\pi(1-g)}\left(\frac{K'+4/3\mu'}{\mu\alpha}\right)\right]}, \quad (4a)$$

$$\Delta_T = \frac{16e}{3(3-2g)\left[1+\frac{4}{\pi(3-2g)}\left(\frac{\mu'}{\mu\alpha}\right)\right]}, \quad (4b)$$

where, $g=\mu/(\lambda+2\mu)$. e is the crack density, and α is aspect ratio. K' and μ' are parameters of fillings in fractures. We assume K' = 0 and μ'=0 when adding fractures into isotropic dry rock.

Step 4: Calculating of moduli and density of mixture of fluid using Wood formula (Wood, 1955):

$$\frac{1}{K_R}=\sum_{i=1}^{N}\frac{f_i}{K_i}, \quad (5a)$$

$$\rho=\sum_{i=1}^{N}f_i\rho_i, \quad (5b)$$

where, K_R is the Reuss (isostress) average of the composite, ρ is density; f_i, K_i and ρ_i are the volume fraction, bulk moduli, and densities of the phases, respectively.

Step 5: Fluid substitution in anisotropic rock. Gurevich (2003) proposed a method to calculate the elastic matrix of fractured rock. In this paper, according to the formula derived by Brown et al. (1975), we calculate the elastic matrix to estimate the moduli of saturated rock:

$$c_{ijkl}^{sat}=c_{ijkl}^{dry}+\frac{\left(K_0\sigma_{ij}-c_{ijaa}^{dry}/3\right)\left(K_0\sigma_{kl}-c_{bbkl}^{dry}/3\right)}{\left(K_0/K_{fl}\right)\phi\left(K_0-K_{fl}\right)+\left(K_0-c_{ccdd}^{dry}/9\right)}, \quad (6)$$

where c_{ijkl}^{dry} is the effective elastic stiffness element of dry rock, c_{ijkl}^{sat} is the effective elastic stiffness element of rock saturated with pore fluid, K_0 is the mineral bulk modulus, K_{fl} is the fluid bulk modulus, and ϕ is porosity.

$$\sigma_{ij}=\begin{cases}1, & i=j,\\ 0, & i\neq j.\end{cases} \quad (7)$$

Huang et al. (2013) presented a new formula to describe the relationship between elastic matrix and fracture weaknesses:

$$\begin{aligned}
C_{11}^{sat}&=(\lambda+2\mu)(1-\Delta_N)\\
&+\frac{\left(K_0-K_{iso}^{dry}+\Delta_N K_{iso}^{dry}\right)^2}{\left(K_0/K_{fl}\right)\phi\left(K_0-K_{fl}\right)+K_0-K_{iso}^{dry}\left(1-\Delta_N K_{iso}^{dry}/(\lambda+2\mu)\right)},\\
C_{33}^{sat}&=(\lambda+2\mu)\left(1-\frac{\lambda^2\Delta_N}{(\lambda+2\mu)^2}\right)\\
&+\frac{\left(K_0-K_{iso}^{dry}+\lambda\Delta_N K_{iso}^{dry}/(\lambda+2\mu)\right)^2}{\left(K_0/K_{fl}\right)\phi\left(K_0-K_{fl}\right)+K_0-K_{iso}^{dry}\left(1-\Delta_N K_{iso}^{dry}/(\lambda+2\mu)\right)},\\
C_{44}^{sat}&=\mu,\\
C_{55}^{sat}&=\mu(1-\Delta_T),
\end{aligned} \quad (8)$$

where C_{11}^{sat}, C_{33}^{sat}, C_{44}^{sat} and C_{55}^{sat} are elastic parameters of saturated fractured rock, and K_{iso}^{dry} is bulk modulus of isotropic dry rock.

Step 6: Estimating P-wave velocity, S-wave velocity and fracture weaknesses. According to the definition of anisotropic parameters proposed by Thomsen (1986), we may estimate P- and S-wave velocities of saturated fractured rock:

$$\alpha=\sqrt{\frac{C_{33}^{sat}}{\rho}},\ \beta=\sqrt{\frac{C_{55}^{sat}}{\rho}}. \quad (9)$$

Eq. (10) describes the relationship between anisotropic parameters and fracture weaknesses (Bakulin et al., 2000):

$$\begin{aligned}
\varepsilon^{(V)}&=-2g(1-g)\Delta_N,\\
\delta^{(V)}&=-2g\left[(1-2g)\Delta_N+\Delta_T\right],\\
\gamma&=\frac{\Delta_T}{2}.
\end{aligned} \quad (10)$$

Using eq. (11), we may estimate weaknesses of saturated fractured rock:

$$\begin{aligned}
\Delta_N&=\frac{C_{33}^{sat}\left(C_{11}^{sat}-C_{33}^{sat}\right)}{4C_{55}^{sat}\left(C_{55}^{sat}-C_{33}^{sat}\right)},\\
\Delta_T&=2\frac{C_{55}^{sat}-C_{44}^{sat}}{2C_{44}^{sat}}.
\end{aligned} \quad (11)$$

We develop the fractured carbonate rock physics model proposed by Zhang et al. (2013). In the process of constructing the model, we use linear slip model to describe the effect of fractures, and calculate Δ_N and Δ_T of fractured dry rock ($K'=0$ and $\mu'=0$). We utilize eq. (8) to calculate elastic matrix of saturated fractured rock. The estimation of velocities and fracture weaknesses from well-logging data may be the initial constraint for the derivation of reflection coefficient approximate formula and seismic inversion. In addition, using our model to estimate parameters from well-logging data may help to reduce the error introduced in the transformation from anisotropic parame-

ters to fracture weaknesses.

1.2 The sensitivity of fracture weaknesses

In this part, we mainly present the relationship between fracture weaknesses and fracture parameters (fracture density and fillings in fractures), as shown in Figure 2. This may reveal the importance of estimating fracture weaknesses and lay a foundation for seismic inversion.

Accord to eq. (10), we analyze the characteristic of fracture weaknesses variation with fracture density and fillings. Figure 2 ((a), (b)), ((c), (d)) and ((e), (f)) are the relationship between fracture weaknesses and S-wave to P-wave velocity ratio when fractures are saturated with water, oil and gas, respectively. From Figure 2, we may find Δ_N and Δ_T increase with fracture density. Δ_N changes most obviously when fractures are full of gas, followed by oil-filled fractures, and finally water-saturated fractures. However, the differences of Δ_T changes among gas-filled fractures, oil-filled and water-filled fractures are small. Hence, we may predict fracture density and the type of fracture fillings after estimating Δ_N and Δ_T by adopting AVAZ inversion method.

2 AVAZ inversion for fracture weaknesses

2.1 Reflection coefficient approximate equation containing fracture weaknesses

Rüger (1996) proposed the P-P wave reflection coefficient for an isotropic half space over an anisotropic half space:

$$\begin{aligned} R_{\mathrm{PP}}(\theta,\phi) &= \frac{1}{2}\frac{\Delta Z}{\overline{Z}} \\ &+\frac{1}{2}\left\{\frac{\Delta\alpha}{\overline{\alpha}}-\left(\frac{2\overline{\beta}}{\overline{\alpha}}\right)^2\frac{\Delta G}{\overline{G}}+\left[\Delta\delta^{(\mathrm{V})}+2\left(\frac{2\overline{\beta}}{\overline{\alpha}}\right)^2\Delta\gamma\right]\cos^2\phi\right\} \\ &\cdot\sin^2\theta+\frac{1}{2}\left\{\frac{\Delta\alpha}{\overline{\alpha}}+\Delta\varepsilon^{(\mathrm{V})}\cos^4\phi+\Delta\delta^{(\mathrm{V})}\sin^2\phi\cos^2\phi\right\} \\ &\cdot\sin^2\theta\tan^2\theta, \end{aligned} \tag{12}$$

where, $G=\rho\beta^2$, $Z=\rho\alpha$; θ is the incidence angle, and ϕ is azimuth angle; α, β and ρ are P-wave velocity, S-wave velocity and density, respectively; $\Delta\alpha/\overline{\alpha}$ is P-wave reflection coefficient; $\Delta\delta^{(\mathrm{V})}$, $\Delta\varepsilon^{(\mathrm{V})}$ and $\Delta\gamma$ are the different in anisotropic parameters between the upper and lower layers.

A new formula which contains fracture weaknesses is derived at small incident angle:

$$\begin{aligned} R_{\mathrm{PP}}(\theta,\phi) &= \sec^2\theta R_{\mathrm{P}}-8g\sin^2\theta R_{\mathrm{S}} \\ &-\left(g\cos^2\phi\sin^2\theta\right)(1-2g)R_{\Delta_{\mathrm{N}}}+\left(g\cos^2\phi\sin^2\theta\right)R_{\Delta_{\mathrm{T}}}, \end{aligned} \tag{13}$$

where, $R_{\mathrm{P}}=\dfrac{I_{\mathrm{P2}}-I_{\mathrm{P1}}}{I_{\mathrm{P2}}+I_{\mathrm{P1}}}=\dfrac{1}{2}\dfrac{\Delta I_{\mathrm{P}}}{\overline{I_{\mathrm{P}}}}$, $R_{\mathrm{S}}=\dfrac{I_{\mathrm{S2}}-I_{\mathrm{S1}}}{I_{\mathrm{S2}}+I_{\mathrm{S1}}}=\dfrac{1}{2}\dfrac{\Delta I_{\mathrm{S}}}{\overline{I_{\mathrm{S}}}}$, $R_{\Delta_{\mathrm{N}}}=\Delta_{\mathrm{N2}}-\Delta_{\mathrm{N1}}$, $R_{\Delta_{\mathrm{T}}}=\Delta_{\mathrm{T2}}-\Delta_{\mathrm{T1}}$; I_{P1}, I_{P2}, I_{S1} and I_{S2} are P-wave and S-wave impedances of the upper and lower layers, respectively; Δ_{N1}, Δ_{N2}, Δ_{T1} and Δ_{T2} are the vertical and tangential weaknesses of the upper and lower layers, respectively.

2.2 AVAZ inversion for elastic parameters and fracture weaknesses

Eq. (13) shows the reflection coefficient of fractured rock is influenced by incident and azimuthal angles. For *n* offsets and *m* azimuthal angles, it may be written as

$$\begin{aligned} \begin{bmatrix} seis(\theta_1,\phi_1) \\ seis(\theta_2,\phi_2) \\ \vdots \\ seis(\theta_n,\phi_m) \end{bmatrix} &= wvlt\cdot\begin{bmatrix} R_{\mathrm{pp}}(\theta_1,\phi_1) \\ R_{\mathrm{pp}}(\theta_2,\phi_2) \\ \vdots \\ R_{\mathrm{pp}}(\theta_n,\phi_m) \end{bmatrix} \\ &= wvlt\cdot\begin{bmatrix} c_1(\theta_1) & c_2(\theta_1) & c_3(\theta_1,\phi_1) & c_4(\theta_1,\phi_1) \\ c_1(\theta_2) & c_2(\theta_2) & c_3(\theta_2,\phi_2) & c_4(\theta_2,\phi_2) \\ \vdots & \vdots & \vdots & \vdots \\ c_1(\theta_n) & c_2(\theta_n) & c_3(\theta_n,\phi_m) & c_4(\theta_n,\phi_m) \end{bmatrix}\begin{bmatrix} R_{\mathrm{P}} \\ R_{\mathrm{S}} \\ R_{\Delta_{\mathrm{N}}} \\ R_{\Delta_{\mathrm{T}}} \end{bmatrix}, \end{aligned} \tag{14}$$

where, *seis* is seismic data, *wvlt* is wavelet matrix,

$c_1(\theta)=\sec^2\theta$, $c_2(\theta)=-8g\sin^2\theta$,

$c_3(\theta,\phi)=-\left(g\cos^2\phi\sin^2\theta\right)(1-2g)$,

$c_4(\theta,\phi)=g\cos^2\phi\sin^2\theta$.

In order to obtain R_{P}, R_{S}, $R_{\Delta_{\mathrm{N}}}$ and $R_{\Delta_{\mathrm{T}}}$, eq. (14) may be simplified to

$$d=GX, \tag{15}$$

where,

$$d=\begin{bmatrix} seis(\theta_1,\phi_1) \\ seis(\theta_2,\phi_2) \\ \vdots \\ seis(\theta_n,\phi_m) \end{bmatrix},$$

$$G=wvlt\cdot\begin{bmatrix} c_1(\theta_1) & c_2(\theta_1) & c_3(\theta_1,\phi_1) & c_4(\theta_1,\phi_1) \\ c_1(\theta_2) & c_2(\theta_2) & c_3(\theta_2,\phi_2) & c_4(\theta_2,\phi_2) \\ \vdots & \vdots & \vdots & \vdots \\ c_1(\theta_n) & c_2(\theta_n) & c_3(\theta_n,\phi_m) & c_4(\theta_n,\phi_m) \end{bmatrix},$$

$$X=\begin{bmatrix} R_{\mathrm{P}} \\ R_{\mathrm{S}} \\ R_{\Delta_{\mathrm{N}}} \\ R_{\Delta_{\mathrm{T}}} \end{bmatrix}.$$

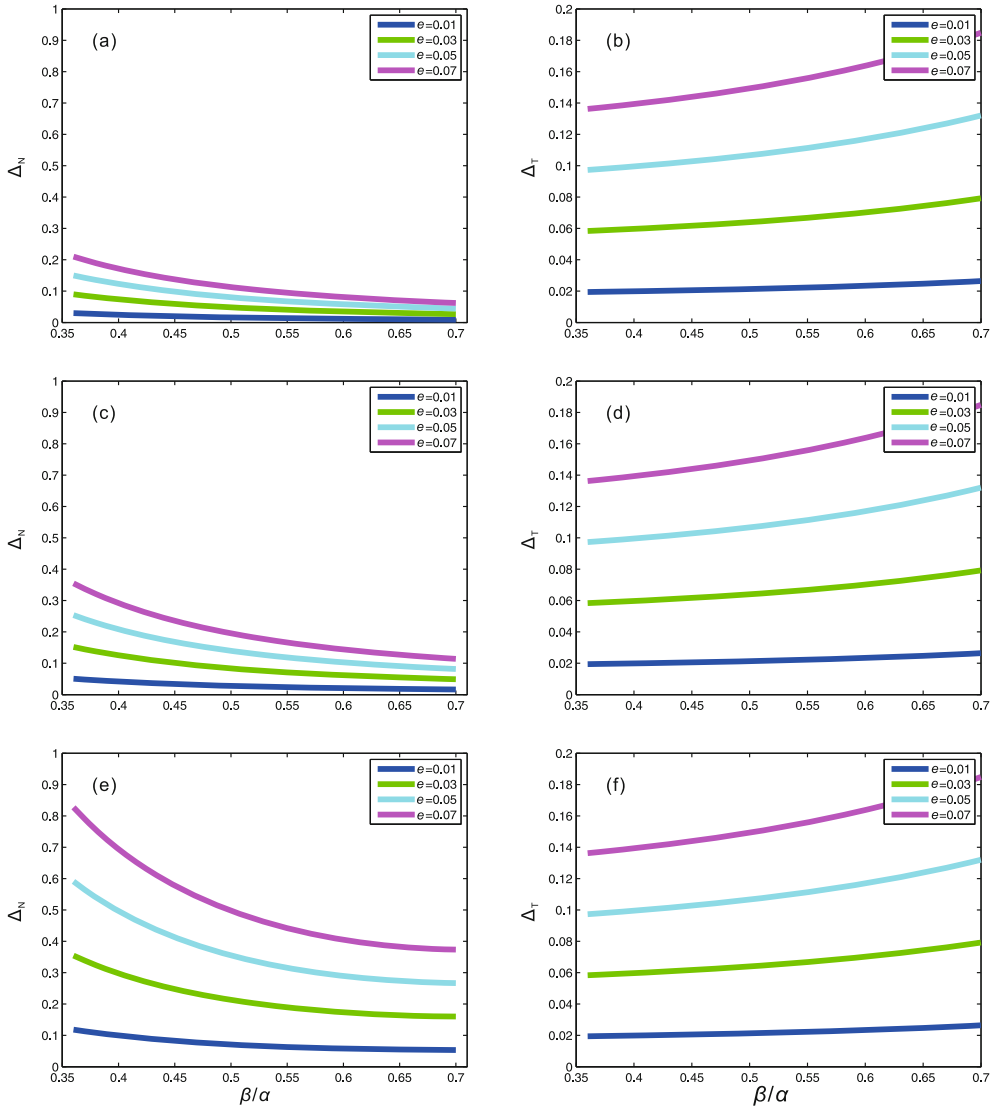

Figure 2 The relationship between fracture rock physics parameters and fracture density and fillings.

By using damped least squares method, we get

$$X = \text{mod\_}X + \left[G^T G + \sigma I\right]^{-1} G^T (d - G \cdot \text{mod\_}X), \quad (16)$$

where $\text{mod\_}X$ represents the initial model which may be calculated by using rock physics model. G^T is transpose of matrix G. σ is damping factor. I is an identity matrix. The choice of damping factor depends mainly on experiments (Yang, 1997). There are many methods about the selection of damping factor. The very useful one is using the covariance matrix of random noise and the inverse covariance matrix of unknown parameters to calculate the damping factor (Downton, 2005).

3 Example

Well-logging and seismic data from fractured carbonate reservoirs are used to verify our method. We first estimate S-wave velocity and fracture weaknesses by using our rock physics effective model, then utilize azimuthal seismic dataset to estimate elastic parameters and fracture weaknesses of the target area.

3.1 Velocities and fracture weaknesses estimation

Acoustic slowness, density, porosity, clay content and water saturation curves of well A are necessary when we estimate velocities and fracture weaknesses. Figure 3(a) is the estimated results of P- and S-wave velocities, and Figure 3(b) is the estimated fracture weaknesses.

From Figure 3, we find the estimated P-wave velocity has a good match with real well-logging data, and the estimated fracture weaknesses may help to predict the location of fractures. By analyzing the characteristic of the estimated results, we also find the value of P- and S-wave velocities is

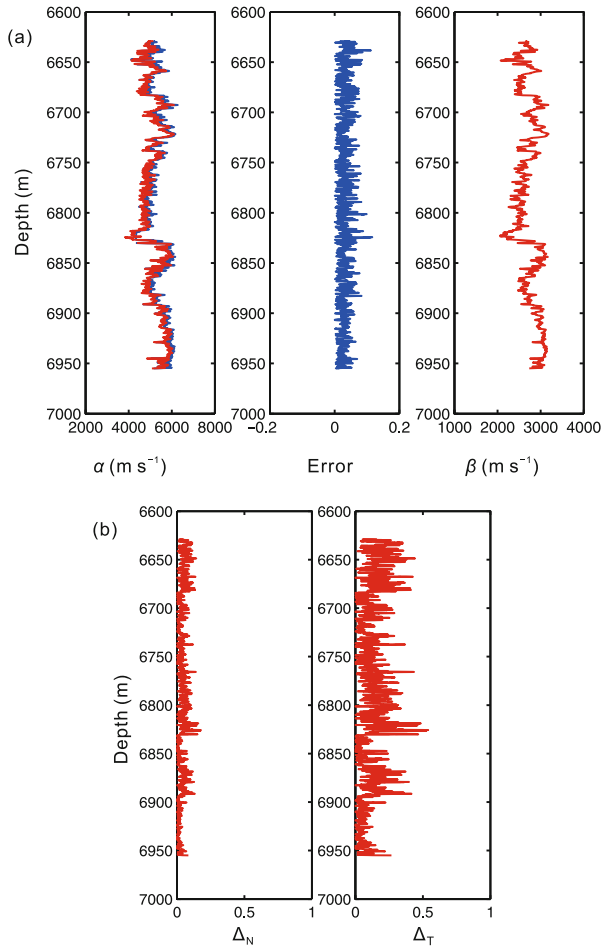

Figure 3 The estimation of velocities and fracture weaknesses. (a) The comparison between estimated velocity and true value, the red line means the estimated result, the blue line means the true value. (b) Fracture weaknesses parameter estimated results.

small and the value of fracture weaknesses is large in fractured layers.

3.2 The analysis of reflection coefficient comparison

The estimated results of well A are used to generate synthetic seismic data with 45 Hz Ricker wavelet. Figure 4 gives the composite show of the synthetic common midpoint profile generated by using extended anisotropic Zoeppritz equation (Schoenberg et al., 1992) and our simplified equation. Figure 4 shows that two profiles match well until the incident angle is around 30 degree.

3.3 AVAZ inversion for elastic parameters and fracture weaknesses

We first verify AVAZ inversion method on synthetic seismic data. To test the stability of the inversion method, we add random noise to the synthetic traces, with different signal-to-noise ratio (S/N), and the S/N is 4 and 1, respectively (Figure 5). Figure 6 shows original and inverted P-wave

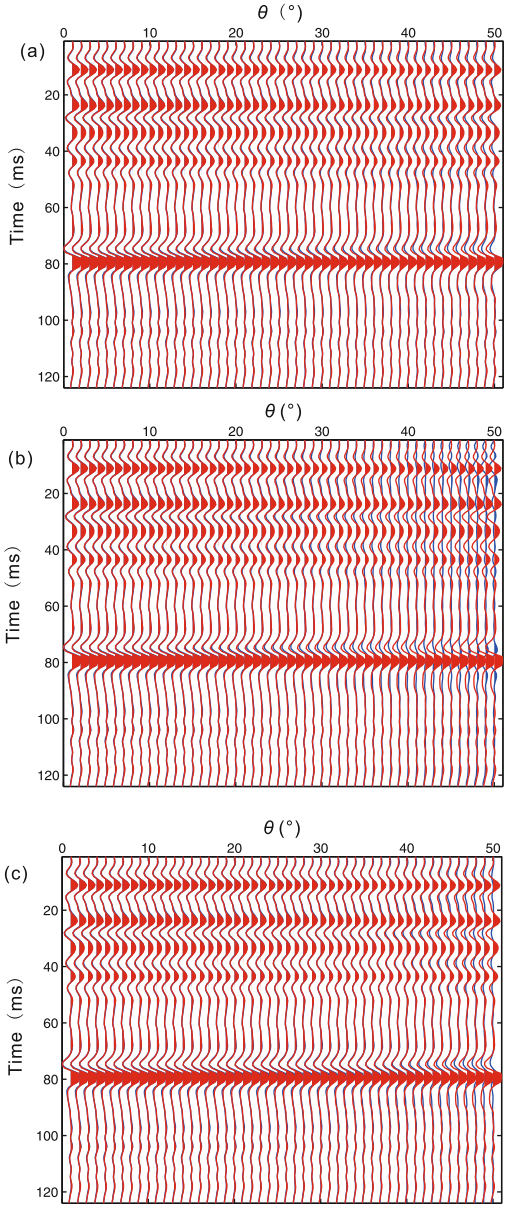

Figure 4 Synthetic data generated by using exact equation and our approximate equation. (a) Azimuthal angle is 0°, (b) angle is 60°, (c) azimuthal angle is 120°. The red line means the approximate equation, the blue line means the exact equation.

impedance, S-wave impedance, the normal weakness and the tangential weakness with different S/N. We perform the inversion with eq. (16). It is easy to demonstrate that the P-wave impedance, S-wave impedance, the normal weakness and tangential weakness may be estimated well even when S/N ratio is 1.

Real data is used to validate the application of AVAZ inversion method. Figure 7 is real CDP seismic profiles of different azimuthal angles, and Figure 8 is the difference between azimuthal seismic data. From Figure 7 and Figure 8, we may find the difference between azimuthal seismic data is not obvious while the incident angle is small, and the difference will become larger when the incident angle

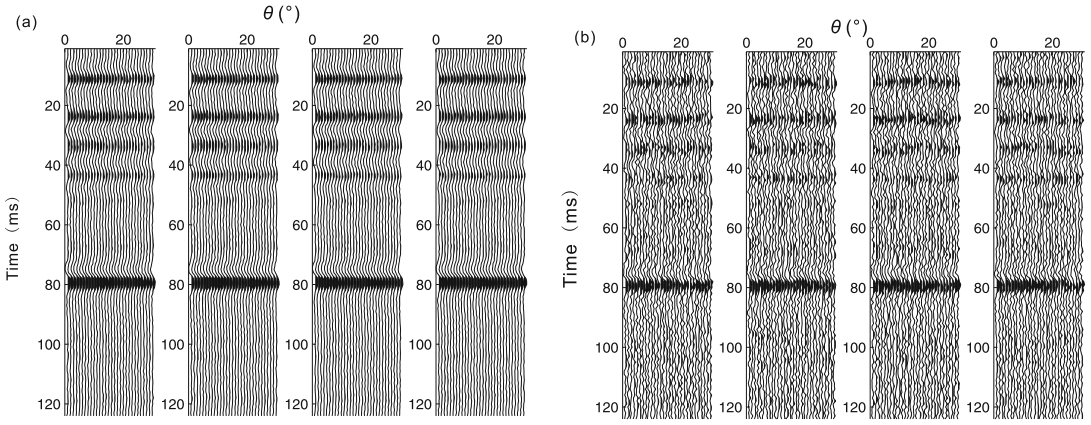

Figure 5 Synthetic profiles with different S/N noise. (a) S/N=4, (b) S/N=1.

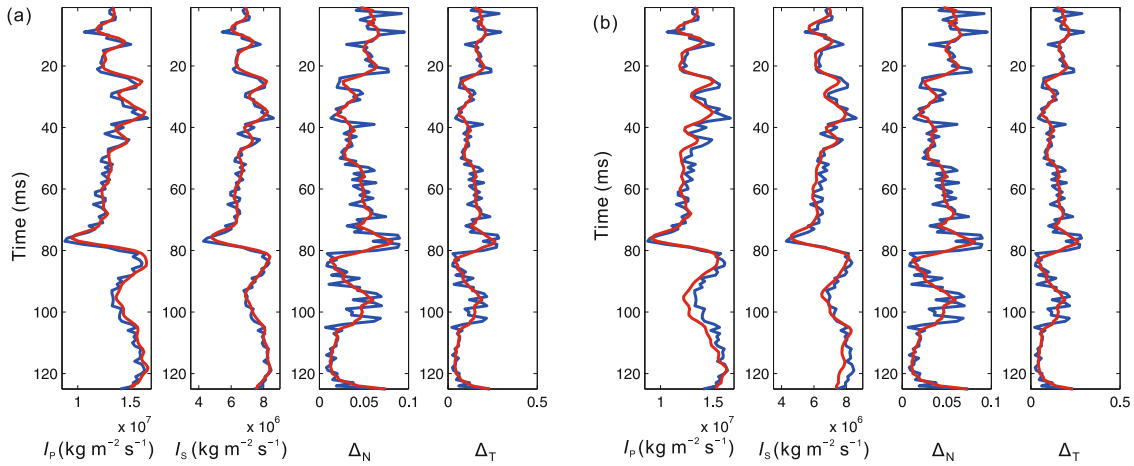

Figure 6 Model inversion result with different noise. The red one means the estimated result, the blue one means the true value.

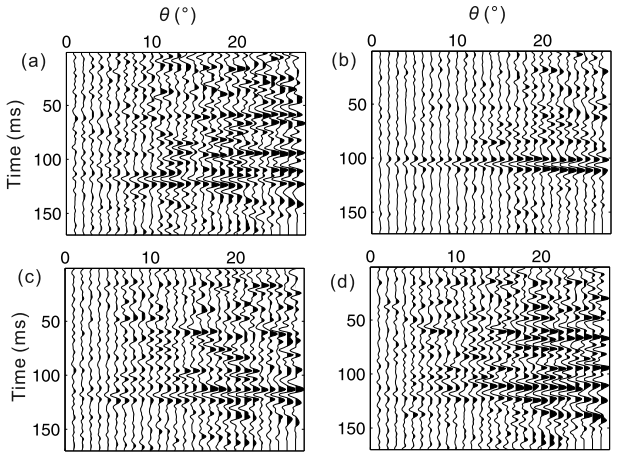

Figure 7 Seismic data of different azimuthal angles.

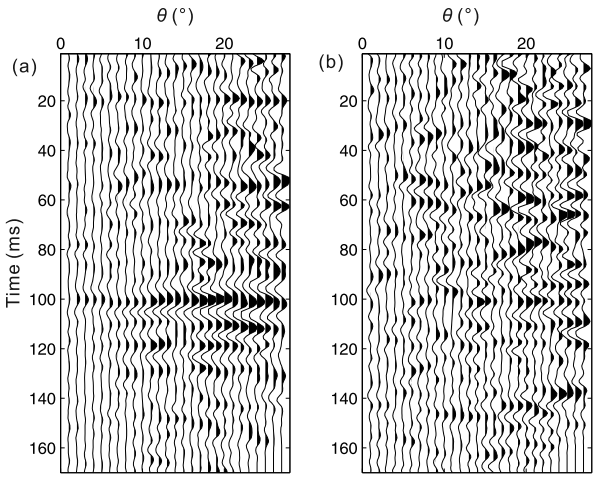

Figure 8 The difference between different azimuthal seismic data. (a) The difference between azimuth 1 and azimuth 2, (b) the difference between azimuth 4 and azimuth 3.

increases.

The estimated P-wave and S-wave impedances, the normal and tangential weaknesses using AVAZ inversion as discussed in this paper are displayed in Figure 9. Figure 9 shows the target reservoir is around 47 ms (CDP 148). From the inverted results, we may find the P-wave impedance and S-wave impedance show low value, and the normal weakness and tangential weakness show high value. This result is

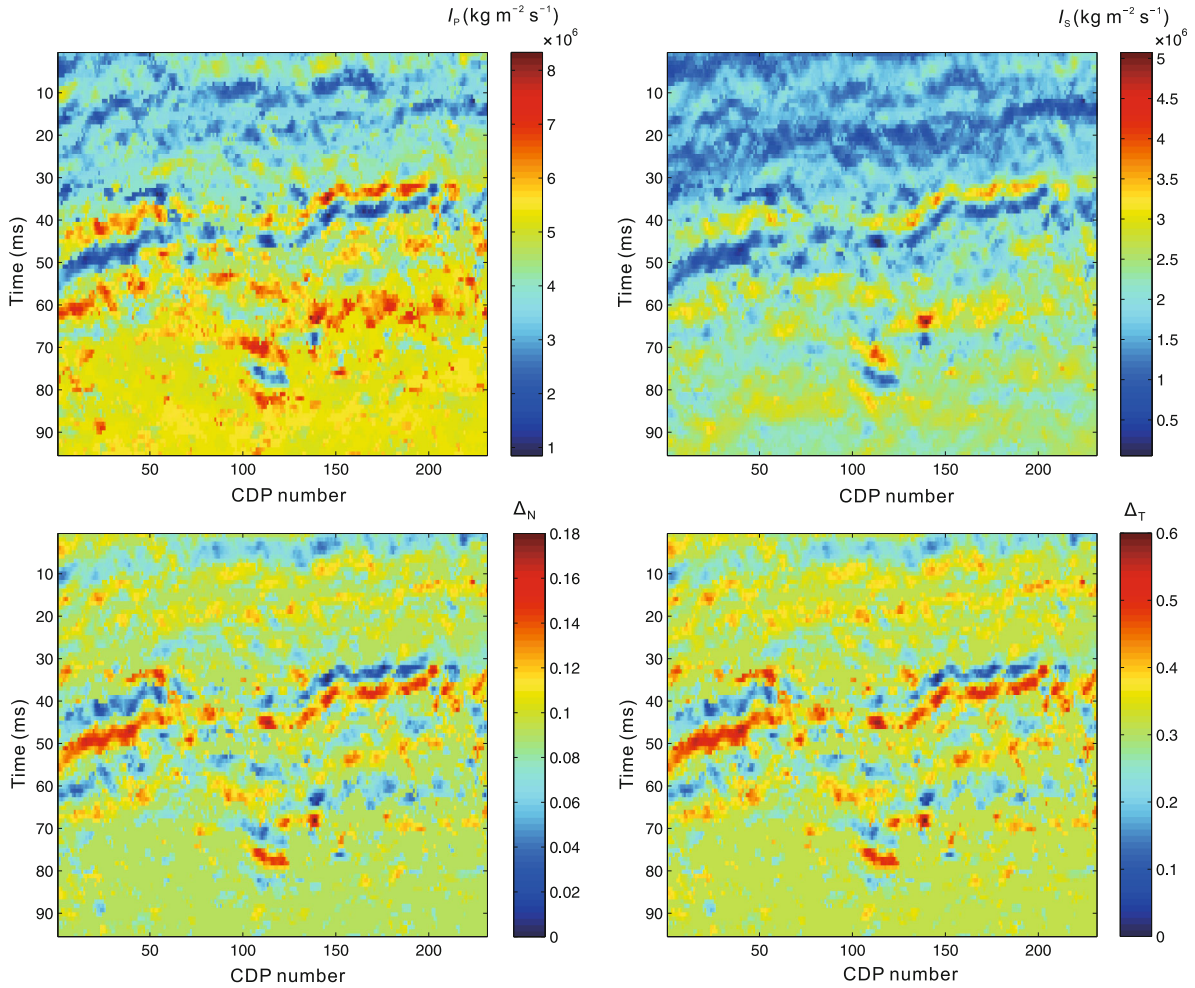

Figure 9 Elastic and fracture weaknesses parameters estimated results.

consistent with the drilling and rock physics analysis result. Although we use azimuthal seismic data to estimate elastic parameters and fracture weaknesses, the influence of random noise is still great, and the accuracy of estimation strongly depends on initial constraint.

Schoenberg et al. (1995) proposed fracture fluid factor. The fluid factor is closely related to the S-wave to P-wave velocity ratio and fracture weaknesses. Hence, the type of fluid filled in fractures may be identified after estimating the P-wave impedance, S-wave impedance and fracture weaknesses.

4 Conclusions

In this paper, a rock physics effective model is proposed to estimate P-wave velocity, S-wave velocity and fracture weaknesses from well-logging data, and a new approximate formula which contains fracture weaknesses parameters is derived for HTI media. The new approach which is based on AVAZ inversion for P-wave impedance, S-wave impedance and facture weaknesses is proposed. At last, well A is used to test the rock physics effective model, and synthetic and real data are used to verify AVAZ inversion method. The results estimated by rock physics effective model may provide an initial constraint for AVAZ inversion, and it may improve the inversion accuracy of the estimation.

The next work will be carried out as follows:

(1) Seismic scattering should be considered when we utilize real data to predict fractured reservoirs in carbonate rock area.

(2) The more stable inversion method should be proposed when processing real data. Well-logging data and rock physics estimated results may be used as the constraint to improve the accuracy of the inversion.

(3) The effective fluid factor is necessary. We may introduce a useful fluid identification factor by using rock physics analysis, and find a new inversion method to estimate the fluid factor.

The work was supported by the National Basic Research Program of China (Grant Nos. 2013CB228604, 2014CB239201), the National Oil and Gas Major Projects of China (Grant No. 2011ZX05014 -001-010HZ), CNPC Innovation Foundation (Grant No. 2011D-5006-0301), the Fundamental

Research Funds for the Central Universities in China (Grant No. 14CX06015A) and SINOPEC Key Laboratory of Geophysics.

Bachrach R, Sengupta M, Salama A, et al. 2009. Reconstruction of the layer anisotropic elastic parameter and high resolution fracture characterization from P-wave data: A case study using seismic inversion and Bayesian rock physics parameter estimation. Geophys Prospect, 57: 253–262

Bakulin A, Grechka V, Tsvankin I. 2000. Estimation of fracture parameters from reflection seismic data—Part I: HTI model due to a single fracture set. Geophysics, 65: 1788–1802

Batzle M, Han D H, Castagna J. 1999. Fluids and frequency dependent seismic velocity of rocks. Seg Tech Prog Exp Abs, 18: 5–8

Batzle M, Han D H, Hofmann R. 2006. Fluid mobility and frequency-dependent seismic velocity—Direct measurements. Geophysics, 71: N1–N9

Biot M A. 1956a. Theory of propagation of elastic waves in a fluid saturated porous solid: A. Low-frequency range. J Acoust Soc Am, 28: 168–179

Biot M A. 1956b. Theory of propagation of elastic waves in a fluid saturated porous solid. B. Higher frequency range. J Acoust Soc Am, 28: 170–191

Brown R, Korringa J. 1975. On the dependence of the elastic properties of a porous rock on the compressibility of the pore fluid. Geophysics, 40: 608–616

Chapman M. 2009. Modeling the effect of multiple sets of mesoscale fractures in porous rock on frequency-dependent anisotropy. Geophysics, 74: D97–D103

Cheng C H. 1978. Seismic velocities in porous rocks: Direct and inverse problems. Doctoral Dissertation. Massachusetts: Massachusetts Institute of Technology

Cheng C H. 1993. Crack models for a transversely anisotropic medium. J Geophys Res, 98: 675–684

Downton J. 2005. Seismic parameter estimation from AVO inversion. Doctoral Dissertation. Alberta: University of Calgary

Downton J, Gray D. 2006. AVAZ parameter uncertainty estimation. Seg Tech Prog Exp Abs, 25: 234–238

Gassmann F. 1951. Uber die elastizitat poroser medien. Vierteljahrsschrift Naturforschenden Gesellschaft Zurich, 96: 1–23

Gurevich B. 2003. Elastic properties of saturated porous rocks with aligned fractures. J Appl Geophys, 54: 203–218

Hill R. 1952. The elastic behavior of crystalline aggregate. Proc Phys Soc, 65: 349–354

Huang L, Jiang T, Omoboya B, et al. 2013. Fluid substitution for an HTI medium. Seg Tech Prog Exp Abs, 32: 2659–2663

Hudson J A. 1981. Wave speeds and attenuation of elastic waves in material containing cracks. Geophys J R Astr Soc, 64: 133–150

Liu E, Martinez A. 2012. Seismic fracture characterization. Netherlands: EAGE Publication

Mallick S, Craft K L, Meister L J, et al. 1998. Determination of the principal directions of azimuthal anisotropy from P-wave seismic data. Geophysics, 63: 692–706

Mavko G, Mukerji T, Dvorkin J. 2009. The Rock Physics Handbook. Cambridge: Cambridge University press.

Quintal B, Schmalholz S M, Podladchikov Y. 2010a. Impact of fluid saturation on the reflection coefficient of a poroelastic layer. Seg Tech Prog Exp Abs, 29: 2730–2735

Quintal B, Steeb H, Frehner M, et al. 2010b. Finite element modeling of seismic attenuation due to fluid flow in partially saturated rocks. Seg Tech Prog Exp Abs, 29: 2564–2569

Quintal B, Schmalholz S M, Podladchikov Y. 2011. Impact of fluid saturation on the reflection coefficient of a poroelastic layer. Geophysics, 76: N1–N12

Quintal B, Steeb H, Frehner M, et al. 2012. Pore fluid effects on S-wave attenuation caused by wave-induced fluid flow. Geophysics, 77: L13–L23

Rüger A. 1996. Reflection coefficient and azimuthal AVO analysis in anisotropic media. Doctoral Dissertation. Colorado: Colorado School of Mines

Rüger A. 1997. P-wave reflection coefficients for transversely isotropic models with vertical and horizontal axis of symmetry. Geophysics, 62: 713–722

Rüger A. 1998. Variation of P-wave reflectivity with offset and azimuth in anisotropic media. Geophysics, 63: 935–947

Sa L M, Yao F C, Di B R, et al. 2011. Seismic response characteristics and identification method of fracture-cavity reservoir (in Chinese). Litholog Reserv, 23: 23–28

Schoenberg M. 1980. Elastic wave behavior across linear slip interface. J Acoust Soc Amer, 68: 1516–1521

Schoenberg M, Douma J. 1988. Elastic wave propagation in media with parallel fractures and aligned cracks. Geophys Prospect, 36: 571–590

Schoenberg M, Helbig K. 1997. Orthorhombic media: Modeling elastic wave behavior in a vertically fractured earth. Geophysics, 62: 1954–1974

Schoenberg M, Muirt F. 1989. A calculus for finely layered anisotropic media. Geophysics, 54: 581–589

Schoenberg M, Protazio J. 1992. 'Zoeppritz' rationalized and generalized to anisotropy. J Seis Expl, 1: 125–144

Schoenberg M, Sayers C M. 1995. Seismic anisotropy of fractured rock. Geophysics, 60: 204–211

Tang W B, Liu L X, Fan G, et al. 2002. Analytic technique of frequency difference for discrimination of cavity fillers (in Chinese). Oil Gas Geol, 23: 41–44

Tang X M. 2011. A unified theory for elastic wave propagation through porous media containing cracks–An extension of Biot's poroelastic wave theory. Sci China Earth Sci, 54: 1441-1452

Thomsen L. 1986. Weak elastic anisotropy. Geophysics, 51: 1954–1966

Teng L. 1998. Seismic and rock physics characterization of fractured reservoirs. Doctoral Dissertation. California: Stanford University

Wood A W. 1955. A Textbook of Sound. New York: McMillan Co

Yao Y, Tang W B. 2003. Theoretical study of detectable cavern-fractured reservoir in weathered Karst of deep carbonate (in Chinese). Oil Geol Prospec, 38: 623–629

Yao Y, Tang W B, Xi X, et al. 2012. Wave field analysis and recognition method of cave reservoir based on numerical simulation (in Chinese). Litholog Reserv, 24: 1–6

Yang W C. 1997. Theory and Methods of Geophysical Inversion (in Chinese). Beijing: Geological Publishing House

Zimmerman R W. 1991. Elastic moduli of a solid containing spherical inclusions. Mech Mater, 12: 17–24

Zhang G Z, Chen H Z, Wang Q, et al. 2013. Estimation of S-wave velocity and anisotropic parameters using fractured carbonate rock physics model (in Chinese). Chin J Geophys, 56: 1707–1715